Sublayer Si atoms as reactive centers in the chemisorption on Si(100): Adsorption of C_2H_2 and C_2H_4

Q. J. Zhang,[1] X. L. Fan,[1,2] W. M. Lau,[2] and Zhi-Feng Liu[1,*]

[1]*Department of Chemistry and Centre for Scientific Modeling and Computation, Chinese University of Hong Kong, Shatin, Hong Kong, China*

[2]*Department of Physics, Chinese University of Hong Kong, Shatin, Hong Kong, China*

The chemisorption of C_2H_2 and C_2H_4 on Si(100) is re-examined by first-principles calculations to sort out the relative importance of the intradimer di-σ and interdimer end-bridge structures. Based on reactive trajectories calculated by *ab initio* molecular dynamics, we identify a reaction channel by the nudged elastic band method, in which a sublayer Si atom is attacked. In the case of C_2H_2 adsorption, this channel is barrierless and plays an important role as an intermediate that leads to the relative abundance of the interdimer end-bridge structure. In the case of C_2H_4, the channel is not as important due to bond-angle distortions. The formation of intradimer di-σ structures is preferred, but interdimer end-bridge structures should be a minor product. Scanning tunnel microscope images and vibrational frequencies are also calculated for the identification of these structures in future experiments.

PACS number(s): 68.43.−h, 34.35.+a, 68.47.Fg

I. INTRODUCTION

The growth of organic layers on Si(100) surface via cycloaddition reaction of unsaturated hydrocarbon molecules onto silicon dimers has been envisioned as a method to make functional semiconductor devices.[1–3] Acetylene (C_2H_2) and ethylene (C_2H_4) are the simplest unsaturated hydrocarbon and have been extensively studied as model compounds for such reactions.[4–27]

It is well understood that silicon dimers are formed on Si(100) after surface reconstruction, with a σ bond and a weak π bond between the two Si atoms, and are therefore considered the reactive centers on the surface. Concerted [2+2] addition on such a dimer should be symmetry forbidden, according to Woodward-Hoffmann rule.[28,29] The existence of intradimer di-σ adsorption products for C_2H_2 and C_2H_4 is commonly thought as due to a two-step asymmetric addition.[29] As shown in Fig. 1(a), a three-atom π complex is formed first, bound by a π dative bond with the electron-deficient down Si atom, and the intradimer di-σ product is

then formed via such a π precursor, which has been identified experimentally by high-resolution electron-energy-loss spectroscopy (HREELS) for C_2H_4 and C_2H_3Br at low temperature around 48–58 K.[30,31] Such a two-step mechanism has been explored by many theoretical calculations.[18,22,32–34]

Another asymmetric mechanism shown in Fig. 1(b) was suggested by Liu and Hamers[35] in the addition of cis- and transdideuteroethylene. It proceeds via a diradical intermediate rather than a π complex, which explains the scanning tunnel microscope (STM) observation of approximately 2% isomerization of two-butene upon adsorption on Si(100).[36] It was supported by theoretical calculations based on a cluster model.[23,37,38] However, such a diradical was not reproduced when a slab model was employed.[22,34]

Recently, a third mechanism was proposed by our group. The concerted [2+2] addition is possible, in violation of the Woodward-Hoffmann symmetry rule.[39] As conceptualized by Hoffmann,[40] electron transfer could be facilitated along the concerted path when the highest occupied molecular orbital (HOMO)-HOMO and lowest unoccupied molecular orbital
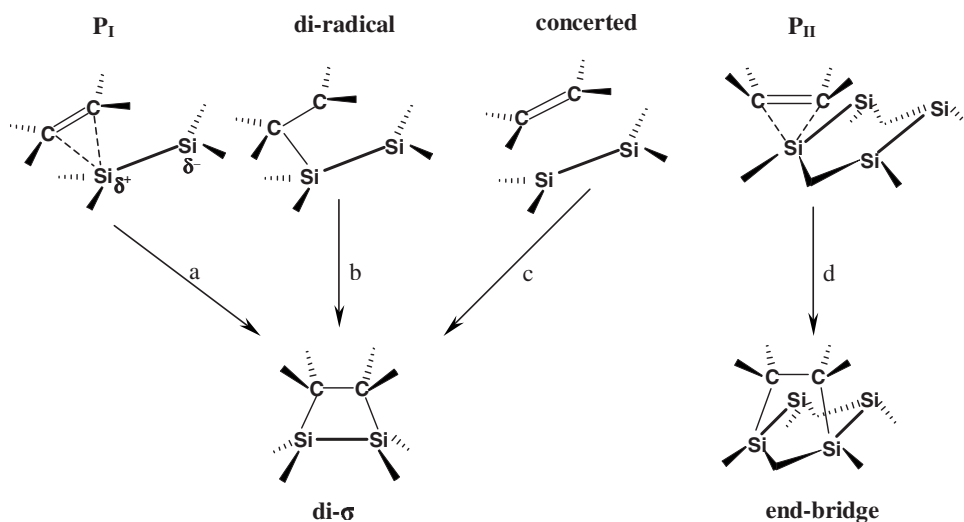

FIG. 1. Schematics for proposed reaction paths for C_2H_4 addition on Si(100) to form di-σ and end-bridge structures. (a) Intradimer [2+2] addition via π complex (P_I); (b) diradical mechanism; and (c) symmetry forbidden [2+2] concerted addition, respectively; (d) interdimer across two adjacent dimer rows via π complex (P_{II}).

(LUMO)-LUMO interactions produce energy levels that cross the Fermi level. However, the concerted mechanism is less important than the π-precursor mechanism because the incoming C≡C bond must be aligned in parallel to the Si dimer.

The addition of unsaturated C≡C bond is not limited to a single Si dimer. It can also be added to one side of two adjacent dimers to produce an interdimer end-bridge structure, which has been observed in recent STM experiments for C_2H_2 but not for C_2H_4.[17,20,24] Furthermore, at low coverage C_2H_2 adsorption, end-bridge structures were found to be more abundant than the intradimer di-σ structures.[17]

Using a slab model, Cho and Kleinman[22] identified the addition barriers for C_2H_2 and C_2H_4 from the π precursors. In the case of C_2H_2, the barrier was almost zero for the intradimer addition and 0.03 eV for the interdimer addition. In the case of C_2H_4, the corresponding barriers were 0.02 and 0.12 eV, respectively. These results raised two questions. First, in the case of C_2H_2, why experimentally is the intradimer di-σ structure less abundant than the interdimer end-bridge structure, although theoretically the barrier in the former case is lower? Second, in the case of C_2H_4, why is the interdimer end-bridge structure not observed in STM experiment[20] despite the fact that a barrier of 0.12 eV should be easily overcome at room temperature?

In the present paper, we report the results of our efforts to find answers to these two questions. Our calculations are also based on a slab model, but real time *ab initio* molecular dynamics (AIMD) are performed to sample reactive trajectories to provide insights into the dynamics of these adsorption. To our surprise, a barrierless reaction channel, with a C_2H_2 molecule attacking a sublayer Si atom, is identified. This channel is responsible for the abundance of the C_2H_2 interdimer end-bridge structure. In addition, our simulations indicate that interdimer end-bridge structures should also be observed for C_2H_4, despite the fact that the reaction channel is not favorable for the C_2H_4 adsorption.

II. COMPUTATIONAL DETAILS

Calculations for the total energy and electronic structure are carried out within density-functional theory (DFT) by using a plane-wave basis set and pseudopotentials for the atomic regions,[41,42] as implemented in the Vienna *ab initio* simulation package (VASP).[43–45] The setup is similar to our previous studies on Si(100) reactions,[34,39,46] with general gradient approximation (GGA) exchange-correlation functional,[47] Vanderbilt ultrasoft pseudopotentials,[43,44,48] and cutoff energy of 300 eV for the plane-wave expansion. The Si(100) surface is modeled by a slab, with a unit cell of the size $7.7 \times 7.7 \times 18.0$ Å^3 containing five Si layers and a vacuum region of 12 Å. The top of the slab is a $p(2 \times 2)$ unit with two asymmetric silicon dimers, while the bottom is saturated by H atoms. This model has been tested and used in a number of previous studies.[18,22,34,39,46] Structural optimization is stopped after the residual force on each atom is less than 0.04 eV/Å. The sampling for the Brillouin zone includes a set of eight special k points. The minimum energy reaction path is mapped out with the nudged elastic band

method, developed by Jónsson and co-workers.[49–51] Vibrational frequencies are calculated using the dynamic matrix method.[52] The STM images are obtained for the electron filled states at −1.5 eV bias and calculated within the Tersoff-Hamman approximation.[53]

To find if there is any dynamic factor that blocks the formation of the interdimer end-bridge structure in C_2H_4 adsorption, AIMD trajectories are simulated using the VASP package, with the potential energy and forces on atoms calculated by density-functional theory as specified above. An optimized π complex structure as shown in Fig. 1 is first equilibrated at 100 K for 3 ps with a time step of 0.3 fs. Structures are randomly chosen from such an equilibration run and used as the starting geometry for trajectory runs with the temperature raised to 300 K, as controlled by a Nose-Hoover thermostat.[54,55] A number of trajectories are also tested at 400 K to see if there is any temperature effect. Each trajectory is terminated after 6000 steps if no reaction takes place. Si and H atoms in the bottom layer are frozen during the AIMD simulations.

With a similar setup, a few trajectories are also simulated for C_2H_2 adsorption. C_2H_2 is more reactive and the simulation temperature is lowered to 60 K for the equilibration run and 150 K for the adsorption run.

III. RESULTS AND DISCUSSIONS

A. Sublayer adsorption of C_2H_2

Two reaction channels have been previously identified for C_2H_2 adsorption on Si(100), producing the intradimer di-σ and the interdimer end-bridge structures, respectively.[22] The most accessible paths are through the π complex, which could actually take two orientations, shown as P_I and P_{II} in Figs. 1(a) and 1(d). As listed in Table I, our calculated adsorption energies are in excellent agreement with the previously reported values, while our calculated reaction barriers are only slightly higher due to a more careful geometry search near the transition region. These results support the previous conclusion that the intradimer addition is favored over the interdimer addition.

AIMD sampling of reactive trajectories turns out to be a surprise. Among the limited number of six trajectories starting from P_{II} precursor performed at 150 K, all lead to a structure termed as the subdi-σ structure in which the C_2H_2 molecule inserts between a sublayer and a dimer Si atom. Its front and side views are shown in Fig. 2(a). The process involves the simultaneous formation of two σ bonds, C1-Si3 and C2-Si2, and the breaking of Si2-Si3 bond. Interestingly, no barrier is found for this reaction, although the adsorption energy at 1.01 eV is lower than that for either the di-σ or end-bridge structures but higher than that for the precursor P_I or P_{II}.

With the breaking of Si2-Si3 bond and the formation of Si2-C2 bond, the π interaction in the Si2-Si2′ dimer is maintained as far as its valence count is concerned, although the Si2-Si2′ distance is increased from 2.36 to 2.45 Å. On the neighboring dimer, the Si1-Si1′ distance is only slightly shortened to 2.33 Å. Some distortions are observed in this structure, most notably in the angle Si3-C1-H1 with a value

TABLE I. The calculated adsorption energies ($E_{ads.}$) and reaction barriers (E_b) of the adsorption structures of C_2H_2 and C_2H_4 on Si(100) at 0.5 and 1.0 ML, respectively. Previous theoretical calculations are listed to provide a comparison.

		$C_2H_2/Si(100)$		$C_2H_4/Si(100)$	
		$E_{ads.}$ (eV)	E_b (eV)	$E_{ads.}$ (eV)	E_b (eV)
	P_I	0.41 (0.41[a])		0.48 (0.47[a])	
	P_{II}	0.41 (0.40[a])		0.47 (0.45[a])	
0.5 ML	subdi-σ	1.01	no barrier	0.23	0.43
	di-σ	2.62 (2.74[b])	0.01 (no barrier[a])	1.92 (1.94[b])	0.07 (0.02[a])
	end-bridge	2.48 (2.61[a])	0.08 (0.03[a])	1.79 (1.82[a])	0.17 (0.12[a])
	$P_{I'}$	0.42		0.31	
1.0 ML	$P_{II'}$	0.50		0.31	
	paired-di-σ	2.77 (2.74[b])	0.02	1.94 (1.89[b])	0.07
	paired-end-bridge	3.05 (2.88[b])	no barrier	2.16 (2.01[b])	0.07

[a]Reference 18.
[b]Reference 22.

of only 106.4° as compared to an ideal sp^2 value of 120°, which is probably responsible for the high energy of this subdi-σ structure, relative to the di-σ and end-bridge structures. Distortions in bond distances and dihedral angles are fairly small, as shown in Fig. 2(a).

It is commonly assumed that the surface dimer is the most reactive site on Si(100) surface and addition reactions typically involve only the surface dimer silicon atoms. But our results indicate that in the case of C_2H_2, the sublayer Si atoms could play a very important role. There is no reaction barrier for the formation of the subdi-σ structure, which makes it an important intermediate in the adsorption process. Not surprisingly, this channel is observed immediately in our very limited number of AIMD simulations.

As shown in Fig. 2(a), there is a barrier of 0.44 eV separating the subdi-σ structure from the more stable end-bridge structure. It indicates that at room temperature it will be converted to the more stable end-bridge structure, while at the same time, it should be possible to isolate such an intermediate at low temperature.

It was reported in an STM experiment[17] that for C_2H_2 the end-bridge structure was more often observed than the di-σ structure, with an approximate ratio of 5:3, in contradiction to the theoretical results which produced a lower barrier and higher adsorption energy for the di-σ structure.[22] Our identification of the subdi-σ structure resolves this puzzle since its formation is barrierless and more favorable than the formation of the di-σ structure. As far as the STM image is concerned, the simulated image for the subdi-σ structure is similar to the image of the end-bridge structure, as shown in Fig. 3. Furthermore, it is an intermediate and is eventually transformed into the end-bridge structure, either by heating or by an STM tip.

B. Sublayer adsorption of C_2H_4

It is natural to ask whether there is a similar sublayer chemisorption structure for C_2H_4. Among the 40 trajectories for the C_2H_4 adsorption on Si(100), also starting from P_{II}, no sublayer adsorption is observed, although a stable subdi-σ structure can be located by geometric optimization at zero temperature. Its adsorption energy, as listed in Table I, is only 0.23 eV. The transformation from the precursor P_{II} to this structure, as shown in Fig. 2(b), is actually endothermic by 0.24 eV. Moreover, there is also a barrier of 0.43 eV for its formation, which is therefore more difficult than the C_2H_2 case.

That C_2H_4 is less reactive than C_2H_2 is expected since there is only one π bond in C_2H_4 compared to two π bonds in C_2H_2. In the C_2H_4 subdi-σ structure, the two H-C-Si angles on C1 atom are only 98.7 and 100.6°, significantly distorted from the ideal value of 109.5° for a sp^3 C, which also contributes to its instability. Overall, it is obvious, as shown in Fig. 2(b), that from the C_2H_4 P_{II} precursor it is easier to form the end-bridge structure than to form the subdi-σ structure in sharp contrast to the case of C_2H_2.

C. Adsorption of C_2H_4

With the subdi-σ structure ruled out for C_2H_4 adsorption, there are still two possible adsorption structures, the intradimer di-σ and the interdimer end-bridge structures. Start-
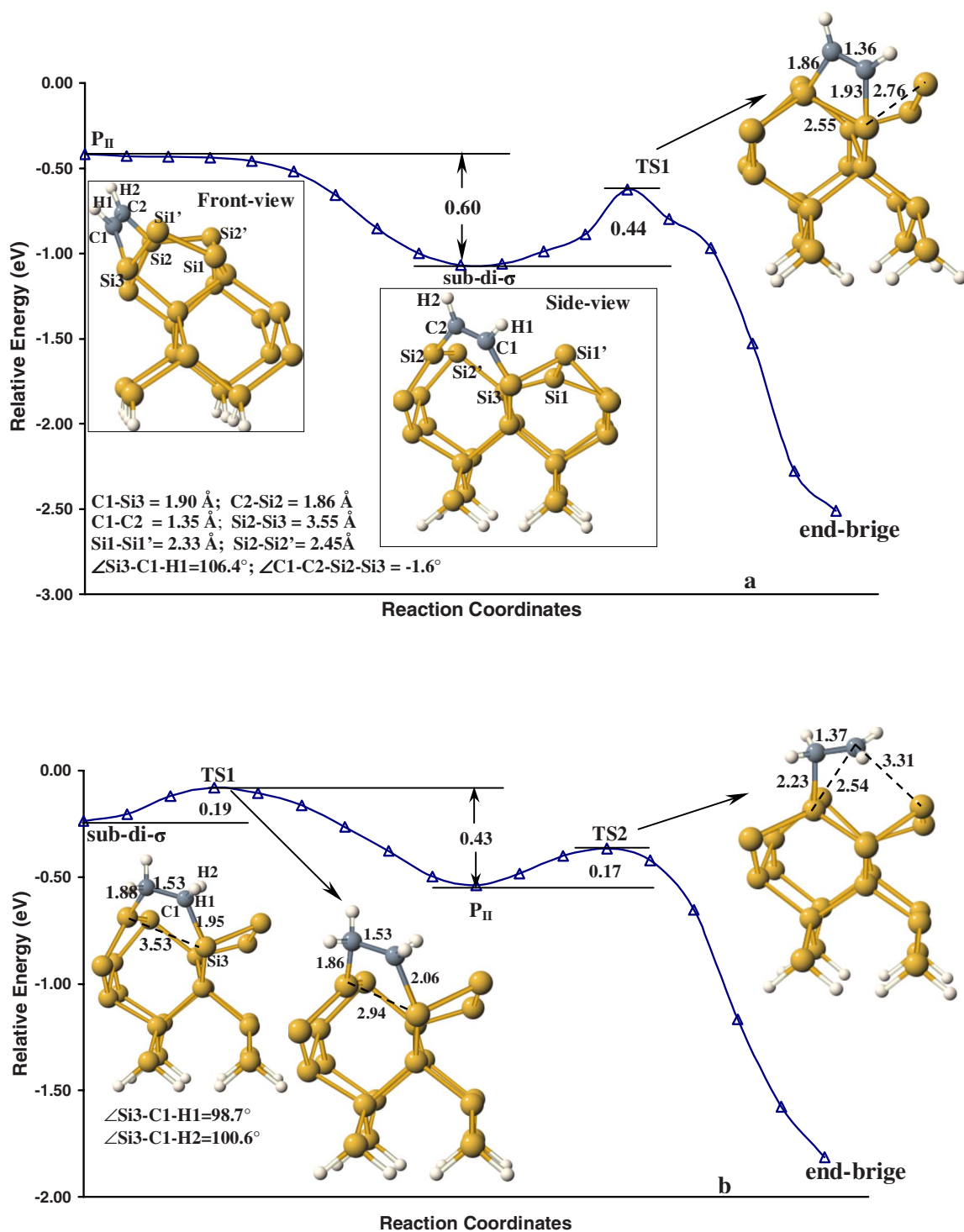
FIG. 2. (Color online) Reaction paths related to the formation of the subdi-σ structure from precursor π complex P_{II}. (a) C_2H_2; (b) C_2H_4. The unit for distances is angstrom.

ing from a π precursor, the barrier is 0.02 eV for the di-σ structure and 0.12 eV for the end-bridge structure, according to the first-principles study by Cho and Kleinman.[22] Our search raises both values to 0.07 and 0.17 eV, respectively, although the difference between the two is again 0.10 eV. There is nonetheless an unresolved puzzle: experimentally, only the di-σ structure is observed, at room temperature.[20] A

difference of 0.10 eV in barrier is hardly enough to account for it.

There is another important experimental difference between the C_2H_4 and C_2H_2 adsorption on Si(100): the π precursor is actually isolated and observed at 48 K for C_2H_4 but not for C_2H_2.[30] This is consistent with the general expectation that C_2H_2 is more reactive, and our results provide fur-
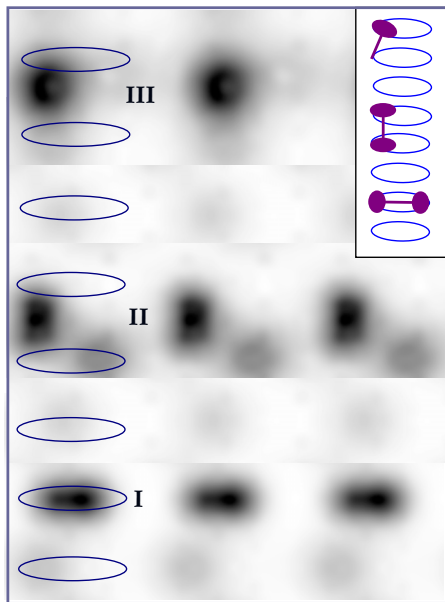
FIG. 3. (Color online) Simulated STM images for electron filled states at -1.5 eV below Fermi surface for C_2H_2 adsorption structures on Si(100). The flat ovals represent Si dimers. The insets show the corresponding adsorption models in schematics.

FIG. 4. (Color online) Simulated STM images for electron filled states at -1.5 eV below Fermi surface for C_2H_2 adsorption structures on Si(100). The flat ovals represent Si dimers. The insets show the corresponding adsorption models in schematics.

ther details for such a difference. An C_2H_2 or C_2H_4 molecule falls onto a dimer Si atom to form a π precursor with random orientation, and relative to the dimer bond, both the parallel P_I and the vertical P_{II} complexes are possible. In the case of C_2H_2, the barrier separating P_I from di-σ is only 0.01 eV, and there is no barrier separating P_{II} from the identified subdi-σ structure. The C_2H_2 π precursor cannot survive even at low temperature (although the subdi-σ structure can). In the case of C_2H_4, the barrier separating P_I from di-σ is 0.07 eV rather than the previously reported 0.02 eV.[22] The barrier is 0.17 eV between P_{II} and end-bridge structures, and 0.43 eV between P_{II} and subdi-σ structures. It is therefore possible to isolate the C_2H_4 π precursors at low temperature.

Based on energy barrier alone, both di-σ and end-bridge structures are possible for C_2H_4 as a difference of 0.1 eV in barrier is not very significant at room temperature. We actually did 40 AIMD trajectories starting from P_{II} at room temperature. About half the trajectories lead to end-bridge structures and half to di-σ structures after an initial rotation to form P_I. According to our calculation, the rotation barrier between P_{II} and P_I is around 0.06 eV. Trajectories starting from P_I precursor all lead to the di-σ structure. While these results indicate that the di-σ structure is preferred, the presence of end-bridge structure cannot be ruled out for the C_2H_4 adsorption. This is in agreement with other theoretical studies.[23,27]

The simulated STM images for C_2H_4 at electron filled state of -1.5 eV are shown in Fig. 4, and there is a clear distinction between the image for the di-σ structure and that for the end-bridge structure. For the former, the depression is aligned along the Si dimer; while for the latter, the depression lies between two adjacent dimers. It may well be worthwhile to check whether such end-bridge structures exist at low coverage.
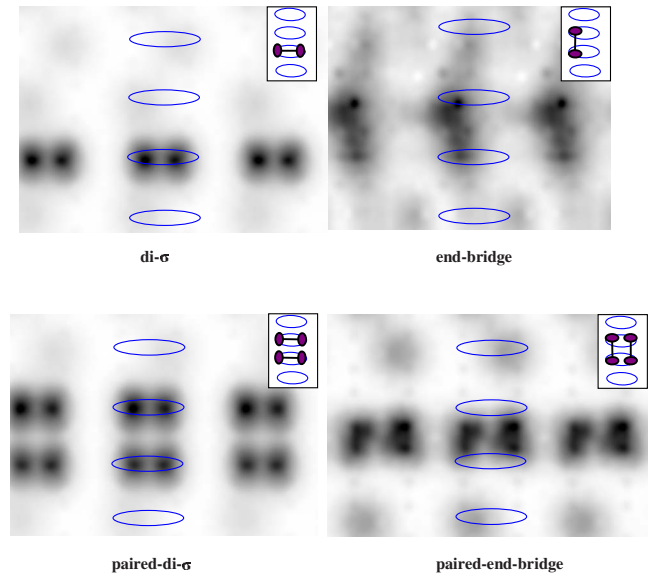
The formation of an end-bridge structure actually produces two Si atoms with dangling bonds, which can be fully saturated by end-bridge adsorption of another C_2H_4 molecule on the same two dimers. The reaction barrier, as we calculated, is 0.07 eV, which is lower than the barrier of 0.17 eV for the first end-bridge adsorption. Therefore at high coverage, it is reasonable to expect that most of the end-bridge structure would be paired, in agreement with previous theoretical results.[22,23] As also shown in Fig. 4, it would be more difficult to tell the difference between the paired-end-bridge structure from the paired-di-σ structure from the STM images since in both cases the depression covers the area of two adjacent dimers.

We also examined the possibility that the C_2H_4 end-bridge structure could go through two C-H bond dissociations, which produce an end-bridge C_2H_2 while the dissociated H atoms saturate the two adjacent Si atoms with dangling bonds. According to our calculations, a stepwise dissociation is more favorable than a concerted one, and the calculated barrier is 1.91 eV for the first C-H dissociation and 0.47 eV for the second. The overall process is exothermic by 0.7 eV. A barrier of 1.91 eV cannot be easily overcome at room temperature. Although an STM tip could induce such a process, the simulated image for this structure is quite similar to the C_2H_4 end-bridge structure as the H atoms on the two Si–H bonds are significantly lower than the C atoms on the end-bridge C_2H_2 structure.

D. Vibrational analysis

Using HREELS, the vibrational spectra for the C_2H_4 adsorption structures have been reported before, identifying the presence of the metastable π-precursor and stable adsorption structures.[30] We have also calculated the vibrational frequencies for both the C_2H_4 and C_2H_2 adsorption structures and

TABLE II. The calculated vibrational frequencies in cm^{-1} for free C$_2$H$_2$ and its adsorption states on Si(100), in comparison with previous results.

	C$_2$H$_2$ (gas)	P_I	P_{II}		di-σ	end-bridge	subdi-σ	di-σ [a]
sym C-H(sp)	3468	3351	3254	sym C-H(sp^2)	3072	3060	3076	3105.9
asym C-H(sp)	3364	3093	3134	asym C-H(sp^2)	3049	3033	2970	3083.1
C≡C	2001	1793	1838	C=C	1461	1434	1490	1492.6
H-bend	752	749	780	CH-rock	1206	1238	1254	1246.4
		660	700					
H-out-of-plane	749	794	736	CH-bend	1013	1091	1096	1056.4
		601	676					
hinder mode		284	220	C-Si	708	680	717	722.9
					675	594	589	697.4

[a]Reference 56.

found excellent agreement with previous experimental and theoretical results.[30,56]

For C$_2$H$_2$ adsorption, the vibrational frequencies for the identified subdi-σ structure are calculated and listed in Table II since it should be possible to isolate such a structure at low temperature. Compared to the di-σ and the end-bridge structures, the most noticeable difference is in the asymmetric C-H stretching. For subdi-σ, its value is 2970 cm^{-1} compared to 3033 cm^{-1} for the end-bridge structure and 3049 cm^{-1} for the di-σ structure. As discussed above, the angle Si3-C1-H1 in the subdi-σ structure is significantly bent from the ideal value, and as a result the C-H bond is weakened, which is reflected on the lower frequency for the asymmetric C-H stretching.

For C$_2$H$_4$ adsorption, the curious question is whether it is possible to tell the difference between the di-σ and the end-bridge structures by vibrational analysis. Unfortunately the answer is negative as the frequencies are almost the same for these two structures, as shown in Table III. The previous HREELS experimental results,[30] together with the theoretical calculated frequencies of the di-σ structure,[56] are also listed in Table III.

IV. CONCLUSIONS

Using *ab initio* molecular dynamics to sample the chemisorption of C$_2$H$_2$/C$_2$H$_4$ on Si(100), we have identified a reaction channel in which the bond between a surface Si and a sublayer Si is broken, while the surface dimers are maintained. It illustrates that surface reactions on Si(100) are not limited to surface dimer atoms.

This channel should play an important role in the adsorption of C$_2$H$_2$ since it is barrierless. It produces an intermediate subdi-σ structure, which is less stable than the end-bridge structure but separated from it by a barrier of 0.44 eV. It is therefore possible to isolate the subdi-σ structure at low temperature. With a distorted H-C-Si angle, its asymmetric C-H stretching frequency is smaller than that for the interdimer end-bridge and intradimer di-σ structures. Its presence contributes to the abundance of end-bridge structures observed in STM experiment.

The subdi-σ structure for C$_2$H$_4$ is less favorable due to larger bond-angle distortions around the carbon atoms. The barrier for its formation is larger than that for either the end-bridge or the di-σ structure. However, AIMD trajectories in-

TABLE III. The calculated frequencies in cm^{-1} for C$_2$H$_4$ adsorption structures on Si (100), in comparison with previous results.

	P_I	P_{II}	Exp.[a]		di-σ	end-bridge	Exp.[a]	di-σ [b]
C-H(sp^2)	3184	3179		C-H(sp^3)	3057	3033		3093.6
	3162	3158			3039	3011		3074.2
	3063	3070			2982	2976		3034.4
	3031	3066	3051		2974	2956	2905	3026.4
C=C	1051	1494	1522	CH$_2$ bend	1397	1390		1457.4
CH$_2$ bend	1411	1390	1394		1388		1401	1443.4
CH$_2$ wag	1264		1280	CH$_2$ wag	1206	1219		1216.6
hinder mode	221	248	220	C-C	920	900	1080	932.2
				CH$_2$ rock	1131	1168		1169.7
					1079	1072	1182	1112.2
				C-Si	669	672		697.6
					630	599	650	657.6

[a]Experimental values from Ref. 30.
[b]Theoretical values from Ref. 56.

dicate that the formation of end-bridge structures should be accessible at room temperature.

*FAX: +852-2603-5057; zfliu@cuhk.edu.hk

[1] R. A. Wolkow, Annu. Rev. Phys. Chem. **50**, 413 (1999).

[2] S. F. Bent, Surf. Sci. **500**, 879 (2002).

[3] X. Lu and M. C. Lin, Int. Rev. Phys. Chem. **21**, 137 (2002).

[4] M. Nishijima, J. Yoshinobu, H. Tsuda, and M. Onchi, Surf. Sci. **192**, 383 (1987).

[5] J. Yoshinobu, H. Tsuda, M. Onchi, and M. Nishijima, J. Chem. Phys. **87**, 7332 (1987).

[6] M. Toscano and N. Russo, J. Mol. Catal. **55**, 101 (1989).

[7] P. A. Taylor, R. M. Wallace, C. C. Cheng, W. H. Weinberg, M. J. Dresser, W. J. Choyke, and J. T. Yates, J. Am. Chem. Soc. **114**, 6754 (1992).

[8] P. L. Cao and R. H. Zhou, J. Phys.: Condens. Matter **5**, 2887 (1993).

[9] C. Huang, W. Widdra, X. S. Wang, and W. H. Weinberg, J. Vac. Sci. Technol. A **11**, 2250 (1993).

[10] M. Kiskinova and J. T. Yates, Surf. Sci. **325**, 1 (1995).

[11] L. Li, C. Tindall, O. Takaoka, Y. Hasegawa, and T. Sakurai, Phys. Rev. B **56**, 4648 (1997).

[12] B. Q. Meng, D. Maroudas, and W. H. Weinberg, Chem. Phys. Lett. **278**, 97 (1997).

[13] F. Matsui, H. W. Yeom, A. Imanishi, K. Isawa, I. Matsuda, and T. Ohta, Surf. Sci. **401**, L413 (1998).

[14] S. H. Xu, Y. Yang, M. Keefe, G. J. Lapeyre, and E. Rotenberg, Phys. Rev. B **60**, 11586 (1999).

[15] D. C. Sorescu and K. D. Jordan, J. Phys. Chem. B **104**, 8259 (2000).

[16] Y. Morikawa, Phys. Rev. B **63**, 033405 (2001).

[17] S. Mezhenny, I. Lyubinetsky, W. J. Choyke, R. A. Wolkow, and J. T. Yates, Chem. Phys. Lett. **344**, 7 (2001).

[18] J. H. Cho, L. Kleinman, C. T. Chan, and K. S. Kim, Phys. Rev. B **63**, 073306 (2001).

[19] P. L. Silvestrelli, F. Toigo, and F. Ancilotto, J. Chem. Phys. **114**, 8539 (2001).

[20] M. Shimomura *et al.*, Surf. Sci. **504**, 19 (2002).

[21] H. W. Yeom, S. Y. Baek, J. W. Kim, H. S. Lee, and H. Koh, Phys. Rev. B **66**, 115308 (2002).

[22] J. H. Cho and L. Kleinman, Phys. Rev. B **69**, 075303 (2004).

[23] X. Lu and M. P. Zhu, Chem. Phys. Lett. **393**, 124 (2004).

[24] C. H. Chung, W. J. Jung, and I. W. Lyo, Phys. Rev. Lett. **97**, 116102 (2006).

[25] G. P. Qin, Y. P. Cai, B. L. Xing, Y. Li, Y. F. Zhang, and J. Q. Li, Chin. J. Chem. **65**, 1305 (2007).

[26] N. Takeuchi, Surf. Sci. **601**, 3361 (2007).

[27] M. Marsili, N. Witkowski, O. Pulci, O. Pluchery, P. L. Silvestrelli, R. D. Sole, and Y. Borensztein, Phys. Rev. B **77**, 125337 (2008).

[28] R. B. Woodward and R. Hoffmann, Angew. Chem., Int. Ed. Engl. **8**, 781 (1969).

[29] Q. Liu and R. Hoffmann, J. Am. Chem. Soc. **117**, 4082 (1995).

[30] M. Nagao, H. Umeyama, K. Mukai, Y. Yamashita, J. Yoshinobu, K. Akagi, and S. Tsuneyuki, J. Am. Chem. Soc. **126**, 9922 (2004).

[31] M. Nagao, K. Mukai, Y. Yamashita, and J. Yoshinobu, J. Phys. Chem. B **108**, 5703 (2004).

[32] J. H. Cho and L. Kleinman, Phys. Rev. B **71**, 125330 (2005).

[33] J. H. Cho, K. S. Kim, and Y. Morikawa, J. Chem. Phys. **124**, 024716 (2006).

[34] Q. J. Zhang, J. L. Wang, and Z. F. Liu, J. Phys. Chem. C **111**, 6365 (2007).

[35] H. B. Liu and R. J. Hamers, J. Am. Chem. Soc. **119**, 7593 (1997).

[36] G. P. Lopinski, D. J. Moffatt, D. D. M. Wayner, and R. A. Wolkow, J. Am. Chem. Soc. **122**, 3548 (2000).

[37] X. Lu, J. Am. Chem. Soc. **125**, 6384 (2003).

[38] Y. Wang, J. Ma, S. Inagaki, and Y. Pei, J. Phys. Chem. B **109**, 5199 (2005).

[39] X. L. Fan, Y. F. Zhang, W. M. Lau, and Z. F. Liu, Phys. Rev. B **72**, 165305 (2005).

[40] R. Hoffmann, Rev. Mod. Phys. **60**, 601 (1988).

[41] M. L. Cohen, Phys. Rep. **110**, 293 (1984).

[42] M. C. Payne, M. P. Teter, D. C. Allan, T. A. Arias, and J. D. Joannopoulos, Rev. Mod. Phys. **64**, 1045 (1992).

[43] G. Kresse and J. Hafner, Phys. Rev. B **48**, 13115 (1993).

[44] G. Kresse and J. Hafner, J. Phys.: Condens. Matter **6**, 8245 (1994).

[45] G. Kresse and J. Furthmuller, Phys. Rev. B **54**, 11169 (1996).

[46] X. L. Fan, Y. F. Zhang, W. M. Lau, and Z. F. Liu, Phys. Rev. Lett. **94**, 016101 (2005).

[47] J. P. Perdew, J. A. Chevary, S. H. Vosko, K. A. Jackson, M. R. Pederson, D. J. Singh, and C. Fiolhais, Phys. Rev. B **46**, 6671 (1992).

[48] D. Vanderbilt, Phys. Rev. B **41**, 7892 (1990).

[49] H. Jonsson, Annu. Rev. Phys. Chem. **51**, 623 (2000).

[50] G. Henkelman, B. P. Uberuaga, and H. Jonsson, J. Chem. Phys. **113**, 9901 (2000).

[51] G. Henkelman and H. Jonsson, J. Chem. Phys. **113**, 9978 (2000).

[52] I. Morrison, J. C. Li, S. Jenkins, S. S. Xantheas, and M. C. Payne, J. Phys. Chem. B **101**, 6146 (1997).

[53] J. Tersoff and D. R. Hamann, Phys. Rev. B **31**, 805 (1985).

[54] S. Nosé, J. Chem. Phys. **81**, 511 (1984).

[55] W. G. Hoover, Phys. Rev. A **31**, 1695 (1985).

[56] N. A. Besley and J. A. Bryan, J. Phys. Chem. C **112**, 4308 (2008).